Four-loop splitting functions in QCD – the gluon-gluon case –

Journal Article

Author(s):
Falcioni, Giulio; Herzog, Franz; Moch, Sven; Pelloni, Andrea; Vogt, Andreas

Publication date:
2025-01

Permanent link:
https://doi.org/https://doi.org/10.3929/ethz-b-000713333

Originally published in:
Physics Letters, Section B: Nuclear, Elementary Particle and High-Energy Physics 860, https://doi.org/10.1016/j.physletb.2024.139194

Phys. Lett. B 860 (2025) 139194

Contents lists available at ScienceDirect

Physics Letters B

journal homepage: www.elsevier.com/locate/physletb

Letter

Four-loop splitting functions in QCD – the gluon-gluon case –

G. Falcioni [a,b,*], F. Herzog [c], S. Moch [d], A. Pelloni [e], A. Vogt [f]

[a] Dipartimento di Fisica, Università di Torino, Via Pietro Giuria 1, 10125 Torino, Italy
[b] Physik-Institut, Universität Zürich, Winterthurerstrasse 190, 8057 Zürich, Switzerland
[c] Higgs Centre for Theoretical Physics, School of Physics and Astronomy, The University of Edinburgh, Edinburgh EH9 3FD, Scotland, UK
[d] II. Institute for Theoretical Physics, Hamburg University Luruper Chaussee 149, D-22761 Hamburg, Germany
[e] Institute for Theoretical Physics, ETH Zürich, 8093 Zürich, Switzerland
[f] Department of Mathematical Sciences, University of Liverpool, Liverpool L69 3BX, United Kingdom

ARTICLE INFO

Editor: G.F. Giudice

ABSTRACT

We have computed the even-N moments $N \leq 20$ of the gluon-gluon splitting function $P_{\rm gg}$ at the fourth order of perturbative QCD via the renormalization of off-shell operator matrix elements. Our results, derived analytically for a general compact simple gauge group, agree with all results obtained for this function so far, in particular with the lowest five moments obtained via structure functions in deep-inelastic scattering. Using our new moments and all available endpoint constraints, we construct improved approximations for the four-loop $P_{\rm gg}(x)$ that should be sufficient for a wide range of collider-physics applications. The N^{3}LO contributions to the scale derivative of the gluon distribution, resulting from these and the corresponding quark-to-gluon splitting functions, amount to 1% or less at $x \gtrsim 10^{-4}$ at a standard reference scale with $\alpha_{\rm s} = 0.2$.

In the next decade, measurements at the Large Hadron Collider (LHC) and the future Electron-Ion Collider (EIC) will reduce the experimental uncertainties of many processes towards 1% [1,2]. For important observables this accuracy requires theoretical calculations at the next-to-next-to-next-to-leading order (N^{3}LO) of perturbative QCD. Fully consistent calculations at this order need, besides the corresponding partonic cross sections, the four-loop contributions to the splitting functions governing the scale dependence (evolution) of the parton distribution functions (PDFs). So far the splitting functions are fully known only to the third order in the strong coupling $\alpha_{\rm s}$ [3,4].

The PDFs and splitting functions can be decomposed into flavour non-singlet (ns) and singlet quantities. Here we focus on the evolution of the singlet quark and gluon distributions,

$$\frac{d}{d\ln\mu^2}\begin{pmatrix} q_{\rm s} \\ g \end{pmatrix} = \begin{pmatrix} P_{\rm qq} & P_{\rm qg} \\ P_{\rm gq} & P_{\rm gg} \end{pmatrix} \otimes \begin{pmatrix} q_{\rm s} \\ g \end{pmatrix} \quad \text{with} \quad P_{\rm ik}(x,\alpha_{\rm s}) = \sum_{n=0} a_{\rm s}^{n+1}\, P_{\rm ik}^{(n)}(x)\,, \tag{1}$$

where $P_{\rm qq}$ is the sum $P_{\rm ns} + P_{\rm ps}$ (pure singlet), $\otimes$ denotes the Mellin convolution in the momentum variable x, and the expansion parameter is chosen as $a_{\rm s} = \alpha_{\rm s}/(4\pi)$. The N^{3}LO contributions $P_{\rm ns}^{(3)}$ have been addressed in ref. [5]; additional results beyond the fully known limit of a large number of colours n_c will be presented elsewhere. The exact x-dependence of $P_{\rm ik}^{(3)}$ in eq. (1) is known only for all leading n_f^3 contributions in the limit of a large number n_f of light flavours [6] and for the n_f^2 parts of $P_{\rm ps}^{(3)}$ and $P_{\rm gq}^{(3)}$ [7,8]. By themselves, however, these results are not relevant for phenomenological analyses – cf. the relative size of the contributions in eq. (5) below.

Exact expressions for the whole matrix in eq. (1) do not appear to be imminent. It is possible, however, to construct approximations by combining the computation of the first even-N Mellin moments,

$$\gamma_{\rm ik}^{(n)}(N) = -\int_0^1 dx\, x^{N-1}\, P_{\rm ik}^{(n)}(x)\,, \tag{2}$$

* Corresponding author.
E-mail address: giulio.falcioni@physik.uzh.ch (G. Falcioni).

https://doi.org/10.1016/j.physletb.2024.139194
Received 21 October 2024; Accepted 9 December 2024

Available online 16 December 2024
0370-2693/

with known constraints in the high-energy (small-x) and threshold (large-x)limits. This was done successfully at N^{2}LO in ref. [9]. In the present case the moments $N \leq 10$ have been computed in refs. [10,11], which is just about sufficient to build first meaningful approximations [11]. With the present means these N^{3}LO calculations, performed via inclusive deep-inelastic scattering (DIS), cannot be extended to higher values of N.

We have therefore undertaken to determine $\gamma_{\rm ik}^{(3)}(N)$ in eq. (2) at $N \leq 20$ in the conceptually more involved, but computationally simpler framework of the operator-product expansion, and to provide approximations of $P_{\rm ik}^{(3)}(x)$ that should be sufficient for most collider-physics applications. The results for $\gamma_{\rm ps}^{(3)}$, $\gamma_{\rm qg}^{(3)}$ and $\gamma_{\rm gq}^{(3)}$ have been published in refs. [12–14]. In this letter, we complete this programme by presenting $\gamma_{\rm gg}^{(3)}(N)$ at $N \leq 20$ and providing accurate approximations of $P_{\rm gg}^{(3)}(x)$.

Here and in refs. [12–14], we have determined the moments (2) as the anomalous dimensions of the gluon and quark twist-2 operators $O_{\rm g}$ and $O_{\rm q}$ via the renormalization of the off-shell operator matrix elements (OMEs) $\mathrm{A_{ij}} = \langle \mathrm{j(p)|O_i|\,j(p)}\rangle$, $\mathrm{i,j = g,q}$. The determination of $\gamma_{\rm gg}^{(3)}$ requires the OMEs $\mathrm{A_{gg}}$ to four loops and $\mathrm{A_{qg}}$ to three loops. The latter contribution enters via the mixing of $O_{\rm q}$ and $O_{\rm g}$. In addition, $O_{\rm g}$ mixes also with unphysical 'alien' operators, see refs. [15,16] and references therein, which we organise in classes of increasing complexity [15].

The operators of the classes O_i^I and O_i^{II}, for $i = A, c$, and O_i^{III}, for $i = A_1, A_2, c$, were already needed for the determination of $\gamma_{\rm gq}^{(3)}$; the associated renormalisation constants were obtained in refs. [14,17]. In principle, the calculation of $\gamma_{\rm gg}$ involves more complicated operators, listed in ref. [15]. However, we find that most of these contributions vanish upon contracting the OMEs with the physical projector [18,19]

$$P_{\mu\nu}(N) = (\Delta\cdot q)^N \left[g_{\mu\nu}(\Delta\cdot q)^2 - (\Delta_\mu q_\nu + \Delta_\nu q_\mu)\,\Delta\cdot q + \Delta_\mu\Delta_\nu\, q^2\right] , \tag{3}$$

where Δ_μ is a lightlike vector and q_μ the momentum of the external gluon. Hence the only new operator that contributes to the renormalization of the physical projection of $\mathrm{A_{gg}}$ is

$$\mathcal{O}_{c_2}^{III} = -d_4^{abcd}\,(\partial\bar{c}^{\,a}) \sum_{i+j+k\,=\,N-4} 3\kappa_{ijk}^{(2)}\left(\partial^i A^b\right)\left(\partial^j A^c\right)\left(\partial^{k+1} c^d\right) . \tag{4}$$

Here $\partial = \Delta^\mu\,\partial_\mu$, $d_4^{abcd} = 1/24\left[\mathrm{Tr}\left(T_A^a T_A^b T_A^c T_A^d\right) + \text{permutations } \{a,b,c,d\}\right]$ with $(T_A^a)_{bc} = i f^{bac}$, where f^{bac} are the structure constant of the gauge group, and A and c denote the gluon and ghost fields. All mixing constants $\kappa_{ijk}^{(2)}$ are given to the relevant perturbative order in ref. [17]. The OMEs $A_{\rm ig}$ are required to three loops for every alien operator i in the classes listed above.

The Feynman diagrams for the calculation of the OMEs, for both physical and alien operators, were generated using QGRAF [20]. They were processed by a FORM [21–23] program that classifies them according to their colour factors [24] and topologies. We have computed the resulting propagator-type integrals for even $N \leq 20$ using an optimized in-house version of FORCER [25]. The $\overline{\rm MS}$ renormalization of the results yields the N^{3}LO anomalous dimensions $\gamma_{\rm gg}^{(3)}(N)$ for any compact simple gauge group in terms of rational numbers and the values ζ_3, ζ_4, ζ_5 of Riemann's ζ-function. Our new results for $N \geq 12$ are given in Appendix A. The numerical values for QCD read

$$\begin{aligned}
\gamma_{\rm gg}^{(3)}(N{=}2) &= \phantom{39876.1233 - {}} 654.462778\, n_f - 245.610620\, n_f^2 + 0.92499097\, n_f^3 ,\\
\gamma_{\rm gg}^{(3)}(N{=}4) &= 39876.1233 - 10103.4511\, n_f + 437.098848\, n_f^2 + 12.9555655\, n_f^3 ,\\
\gamma_{\rm gg}^{(3)}(N{=}6) &= 53563.8435 - 14339.1310\, n_f + 652.777331\, n_f^2 + 16.6541037\, n_f^3 ,\\
\gamma_{\rm gg}^{(3)}(N{=}8) &= 62279.7438 - 17150.6968\, n_f + 785.880613\, n_f^2 + 18.9331031\, n_f^3 ,\\
\gamma_{\rm gg}^{(3)}(N{=}10) &= 68958.7532 - 19307.3854\, n_f + 883.929802\, n_f^2 + 20.6112832\, n_f^3 ,\\
\gamma_{\rm gg}^{(3)}(N{=}12) &= 74473.0024 - 21076.0320\, n_f + 962.264417\, n_f^2 + 21.9511603\, n_f^3 ,\\
\gamma_{\rm gg}^{(3)}(N{=}14) &= 79209.0111 - 22583.5268\, n_f + 1027.80706\, n_f^2 + 23.0713754\, n_f^3 ,\\
\gamma_{\rm gg}^{(3)}(N{=}16) &= 83378.4014 - 23901.3437\, n_f + 1084.30677\, n_f^2 + 24.0362925\, n_f^3 ,\\
\gamma_{\rm gg}^{(3)}(N{=}18) &= 87112.4096 - 25074.2309\, n_f + 1134.04028\, n_f^2 + 24.8850403\, n_f^3 ,\\
\gamma_{\rm gg}^{(3)}(N{=}20) &= 90499.2530 - 26132.2983\, n_f + 1178.50283\, n_f^2 + 25.6433278\, n_f^3 .
\end{aligned} \tag{5}$$

As required by the momentum sum rule, the result for $\gamma_{\rm gg}^{(3)}(N{=}2)$ is minus that for $\gamma_{\rm qg}^{(3)}(N{=}2)$ in ref. [13]. At $N \leq 10$ the results agree with refs. [10,11]. The coefficients of n_f^3 in eq. (5) agree with the all-N results, also computed via DIS, in eq. (3.14) of ref. [6].

Besides the leading large-n_f contributions, all-N expressions for $\gamma_{\rm gg}^{(3)}$ have been obtained until now only for the ζ_4 part, in eq. (12) of ref. [26], and the ζ_5 coefficients of the quartic group invariants [27]. Using our results to $N = 20$, we have now been able to determine at all N the ζ_5 coefficients for all colour factors and the ζ_3 terms of the n_f^2 contributions.

The all-N expressions of the anomalous dimensions up to N^{3}LO – as far as they are known now – can be expressed in terms of powers of simple denominators $1/(N+a) \equiv D_a$ and harmonic sums $S_{\vec{w}}(N)$ [28], see also ref. [29]. Below the denominators will occur mostly, but not exclusively, in the $N \to -N-1$ reciprocity invariant combinations

$$\eta = D_0 - D_1 \equiv \frac{1}{N} - \frac{1}{N+1} , \quad \nu = D_{-1} - D_2 \equiv \frac{1}{N-1} - \frac{1}{N+2} . \tag{6}$$

Note that the results in refs. [6] and [26] are given for a slightly different notation with $\nu = D_{-1}\, D_2$.

The complete all-N form of the ζ_5 contribution to $\gamma_{\rm gg}^{(3)}$ reads

$$\begin{aligned}
\gamma_{gg}(N)\Big|_{\zeta_5} = {}& C_A^4\Big(- 8/27\, N(N+1) - 12016/27 - 1120/3\,\nu - 640/3\,\nu^2 + 3008/9\,\eta + 640\,\eta^2 \\
&+ 1760/3\, S_1 + 640/3\, S_1 \left\{2\nu - 2\eta - S_1\right\}\Big) + d_A^{abcd} d_A^{abcd}/n_a\Big(- 32/9\, N(N+1) - 48064/9 \\
&- 4480\,\nu - 2560\,\nu^2 + 12032/3\,\eta + 7680\,\eta^2 + 7040\, S_1 + 2560\, S_1\left\{2\nu - 2\eta - S_1\right\}\Big)
\end{aligned}$$

$$
\begin{aligned}
&+ n_f\, C_A^3 \big(16/27\, N(N+1) + 272/27 + 1280/9\, \nu + 2384/9\, \eta - 12160/3\, \eta^2 + 160/3\, S_1 \big) \\
&+ n_f\, C_A^2 C_F \big(160 - 5440/3\, \nu + 3280\, \eta + 14720\, \eta^2 + 160\, S_1 \big) + n_f\, C_A C_F^2 \big(2560\, \nu \\
&- 6480\, \eta - 20960\, \eta^2 - 320\, S_1 \big) + n_f\, C_F^3 \big(- 2560/3\, \nu + 2720\, \eta + 10560\, \eta^2 \big) \\
&+ n_f\, d_R^{abcd}\, d_A^{abcd}/n_a \big(128/9\, N(N+1) + 36736/9 + 2560/3\, \nu - 15488/3\, \eta + 6400\, \eta^2 \\
&- 2560\, S_1 \big) + n_f^2 C_A^2 \big(- 8/27\, N(N+1) - 136/27 + 368/9\, \eta - 640/3\, \eta^2 \big) \\
&+ n_f^2 d_R^{abcd}\, d_R^{abcd}/n_a \big(- 128/9\, N(N+1) - 2176/9 + 5888/3\, \eta - 10240\, \eta^2 \big) \,.
\end{aligned} \tag{7}
$$

Here and below we suppress the argument N for brevity. The corresponding n_f^2 terms with ζ_3 are

$$
\begin{aligned}
\gamma_{gg}(N)\Big|_{\zeta_3} \;=\;& n_f^2 C_A^2 \big(- 32/135\, N(N+1) S_{-2} - 104/135 - 114464/405\, \nu - 448/9\, \nu^2 \\
&+ 6364/9\, \eta + 6872/9\, \eta^2 + 192\, \eta^3 - 544/135\, S_{-2} - 448/45\, S_{-2}\, \eta + 640/9\, S_1 \\
&+ 3680/27\, S_1 \nu - 4016/9\, S_1 \eta - 2624/9\, S_1 \eta^2 + 256/3\, S_1 \eta^3 + 64/3\, S_1^2\, \eta\, \{1 - 4\eta\} \big) \\
&+ n_f^2\, C_A C_F \big(32/27\, \delta(N-2) - 160/9 + 3904/9\, \nu + 256/3\, \nu^2 - 11152/9\, \eta - 5728/3\, \eta^2 \\
&- 1472/3\, \eta^3 + 32/3\, \{ 7\, D_{-1} - 7\, D_0 - 5\, D_0^2 - 4\, D_0^3 \} - 640/9\, S_1 - 2432/9\, S_1 \nu + 768\, S_1 \eta \\
&+ 2560/3\, S_1 \eta^2 \big) + n_f^2 C_F^2 \big(176/9 - 2240/27\, \nu - 256/9\, \nu^2 + 480\, \eta + 7264/9\, \eta^2 + 448/3\, \eta^3 \\
&+ 256/3\, \{ -2\, D_{-1} + 2\, D_0 + D_0^2 + 2\, D_0^3 \} + 1280/9\, S_1 \nu - 448\, S_1 \eta - 1408/3\, S_1 \eta^2 \big) \\
&+ n_f^2 d_R^{abcd}\, d_R^{abcd}/n_a \big(- 512/45\, N(N+1) S_{-2} - 7424/45 - 76544/135\, \nu + 4224\, \eta \\
&+ 3840\, \eta^2 - 8704/45\, S_{-2} - 7168/15\, S_{-2}\, \eta + 512/9\, S_1 \nu - 9728/3\, S_1 \eta + 13312/3\, S_1 \eta^2 \\
&+ 4096\, S_1 \eta^3 + 1024\, S_1^2\, \eta\, \{1 - 4\eta\} \big) \,.
\end{aligned} \tag{8}
$$

The above expressions include two structures that do not occur in the three-loop anomalous dimensions [3,4], but enter the coefficient functions for inclusive DIS at this order in α_s [30]. These are the terms with $N(N+1)\{\zeta_5, \zeta_3 S_{-2}\}$, which occur in all non-C_F contributions, and the $\zeta_3\, \delta(N-2)$ term in the $n_f^2 C_A C_F$ part. The latter is also present in $\gamma_{\rm ns}^{(3)}$ [31], $\gamma_{\rm ps}^{(3)}$ [7] and in $\gamma_{\rm gq}^{(3)}$ [8], where it arises from the non-ζ contribution $(N-2)^{-1}\, S_{-2}(N-2)$, corresponding to $x^{-2}\, {\rm H}_{-1,0}(x) = x^{-2}\, [\ln(x) \ln(1+x) + {\rm Li}_2(-x)]$ in x-space, see refs. [32,33].

As already noted in ref. [5], the $\zeta_5\, N(N+1)$ terms suggest contributions $N(N+1)\, f(N)$ with

$$
f(N) \;=\; 5\zeta_5 + 4\zeta_3 S_{-2} - 2S_{-5} - 4S_{-2,-3} + 8S_{-2,-2,1} + 4S_{3,-2} - 4S_{4,1} + 2S_5 \tag{9}
$$

which were first encountered and discussed in ref. [30]. Indeed, the corresponding coefficients in the n_f^2 parts of eq. (7) and in eq. (8) are consistent with eq. (9). The $N(N+1)$ contributions to eq. (7) vanish, separately for the quadratic and quartic group invariants, for the choice of n_f and colour factors that leads to an $\mathcal{N}=1$ supersymmetric theory, see eq. (2.8) of ref. [34].

With eq. (7), all ζ_5 contributions to $\gamma_{\rm ik}^{(3)}(N)$ are now completely known. Their combination $(\gamma_{\rm qq} + \gamma_{\rm gq} - \gamma_{\rm qg} - \gamma_{\rm gg})\big|_{\zeta_5}$ vanishes in the same manner for the above $\mathcal{N}=1$ case. Beyond the results in eq. (8), we have been able to determine the all-N form so far only for the combination of the $\zeta_3\, d_A^{abcd}\, d_A^{abcd}/n_a$ and $\zeta_3\, n_f\, d_R^{abcd}\, d_A^{abcd}/n_a$ contributions that enters the supersymmetric limit. Its $N(N+1)\, S_{-2}$ coefficient also agrees with the presence of the function (9).

The above partial all-N results are of theoretical interest but not relevant to N^{3}LO analyses at the LHC. Until the complete functions $P_{\rm ik}^{(3)}(x)$ become known, such analyses will have to rely on approximations based on the available moments and information about the large-x and small-x limits. With eq. (5) we are now in the position to improve upon the $N \le 10$ based approximations of ref. [11], thus putting $P_{\rm gg}^{(3)}$ on the same footing as $P_{\rm ps}^{(3)}$, $P_{\rm qg}^{(3)}$ and $P_{\rm gq}^{(3)}$ in refs. [12–14].

The large-x behaviour of $P_{\rm gg}^{(3)}(x)$ has been addressed in detail in ref. [11]. It can be written as

$$
P_{\rm gg,\, x\to 1}^{(3)}(x) \;=\; A_{\rm g}^{(4)}/(1-x)_+ \,+\, B_{\rm g}^{(4)}\, \delta(1-x) \,+\, C_{\rm g}^{(4)}\, \ln(1-x) \,-\, A_{\rm g}^{(4)} + D_{\rm g}^{(4)} \tag{10}
$$

up to terms that vanish for $x \to 1$. Here $A_{\rm g}^{(4)}$ denotes the four-loop (lightlike) cusp anomalous dimension [35,36], $B_{\rm g}^{(4)}$ is the corresponding virtual anomalous dimension [37,38], and the coefficients $C_{\rm g}^{(4)}$ and $D_{\rm g}^{(4)}$ are functions of lower-order quantities [5,39]. With the exception of a few n_f^0 and n_f^1 contributions to $B_{\rm g}^{(4)}$, the coefficients in eq. (10) are completely known, see eqs. (15), (16) and (20) of ref. [11]. Their rounded numerical values for QCD are

$$
\begin{aligned}
A_{\rm g}^{(4)} &= 40880.330 \,-\, 11714.246\, n_f \,+\, 440.04876\, n_f^2 \,+\, 7.3627750\, n_f^3 \,, \\
B_{\rm g}^{(4)} &= 68587.64 \pm 0.2 \,-\, 18143.983\, n_f \,+\, 423.81135\, n_f^2 \,+\, 0.90672154\, n_f^3 \,, \\
C_{\rm g}^{(4)} &= 85814.120 \,-\, 13880.515\, n_f \,+\, 135.11111\, n_f^2 \,, \\
D_{\rm g}^{(4)} &= 54482.808 \,-\, 4341.1337\, n_f \,-\, 21.133333\, n_f^2 \,.
\end{aligned} \tag{11}
$$

The uncertainty of the n_f^1 contribution to $B_{\rm g}^{(4)}$ is now negligible for all practical purposes; that of the n_f^0, although less than 10^{-5} of its value, is not irrelevant in the present context.

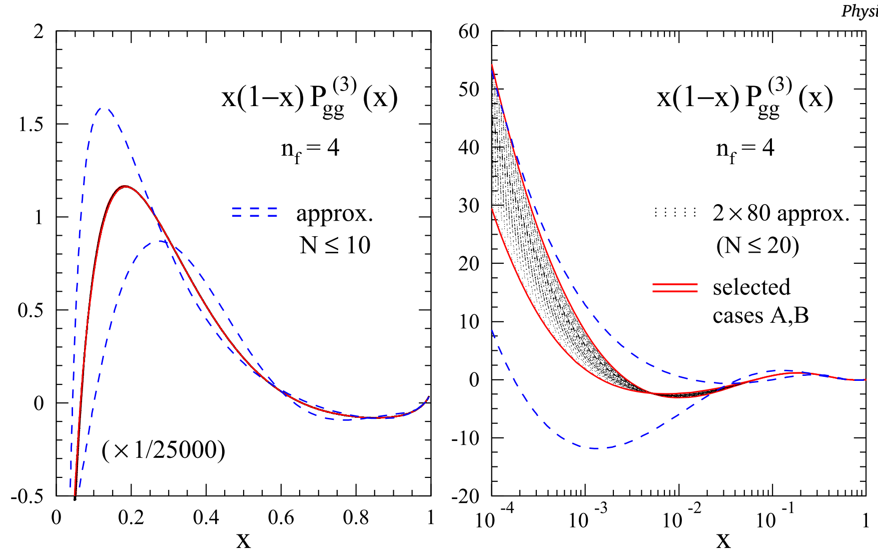

Fig. 1. Two sets of 80 trial functions for the four-loop (N^{3}LO) contribution to the gluon-gluon splitting function at $n_f = 4$. The two cases selected for eq. (15) are shown by the solid (red) lines. Also shown, by the dashed (blue) lines, are the selected approximations of ref. [11] based on only the first 5 even moments.

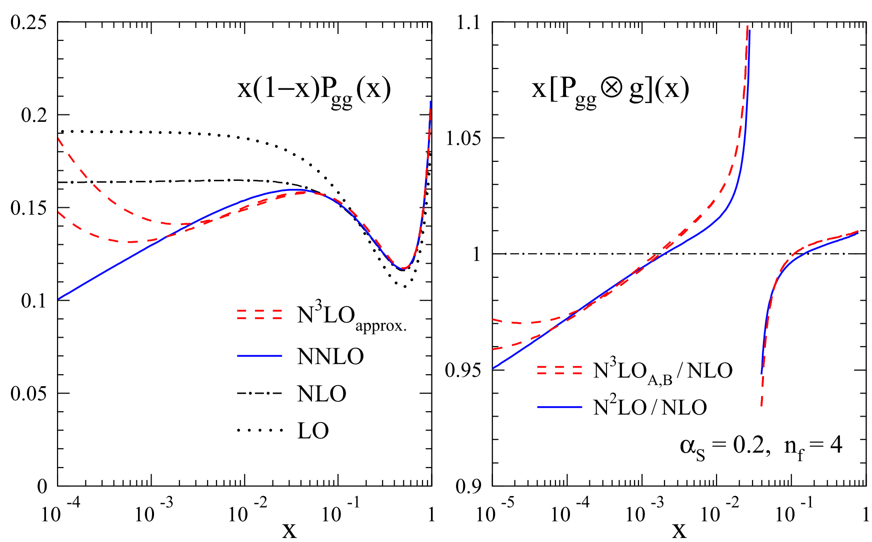

Fig. 2. Left: the perturbative expansion of the splitting functions P_{gg} to N^{3}LO for $n_f = 4$ and $\alpha_s = 0.2$, using eq. (15) for the four-loop contribution. Right: the resulting N^{2}LO and N^{3}LO convolutions with the reference gluon distribution in eq. (18) normalized to the NLO result which changes sign at about $x = 0.03$.

Up to this small uncertainty, the unknown part of $P^{(3)}_{gg}(x)$ vanishes as $x \to 1$, i.e., its behaviour is the same as that for the pure-singlet splitting function in ref. [12]: at large x, the $(1-x)\ln^{\ell}(1-x)$ have been determined for $\ell = 3, 4$ [40]; the coefficients for $\ell = 1, 2$ are unknown. The dominant (BFKL) small-x terms $x^{-1}\ln^m x$ are known for $m = 3$ [41,42] and $m = 2$ [43–46], but not for $m = 1$ and $m = 0$. The sub-dominant small-x terms of the form $\ln^n x$ have been obtained for $n = 4, 5, 6$ [47]; the remaining three coefficients are unknown.

Consequently, the approximations for $P^{(3)}_{gg}$ can be built in basically the same manner as those for $P^{(3)}_{ps}$ in ref. [12]: the seven unknown endpoint functions above are combined with 10 choices of a two-parameter rational function that vanishes as $x \to 1$ and 8 choices of a non-rational interpolating function. In this manner we have built 80 trial functions for both 'extreme' values of $B^{(4)}_g$ in eq. (11), of which we choose two representatives that reflect the remaining uncertainties.

This procedure is illustrated in Fig. 1 for $n_f = 4$. The 80 trial functions are shown as dotted lines. In the left panel their spread is hardly visible, in striking contrast to the uncertainty band, shown by the dashed lines, of the previous approximations based on only five moments [11]. At small-x (right panel), $P^{(3)}_{gg}$ is now well constrained at about $x > 10^{-3}$, which represents an improvement by about one order of magnitude in x. Consequently, the approximation uncertainty is now hardly visible at $x \gtrsim 3 \cdot 10^{-3}$ for the total N^{3}LO splitting function P_{gg} shown in the left part of Fig. 2.

The selected approximations are built up as

$$P^{(3)}_{gg,A/B}(n_f, x) = p^{[n_f]}_{gg,0}(x) + p^{[n_f]}_{gg,A/B}(x)\,, \tag{12}$$

where $p^{[n_f]}_{gg,0}(x)$ collects the known endpoint contributions discussed above. Using the abbreviations $x_1 = 1-x$, $L_1 = \ln(1-x)$, $L_0 = \ln x$, and as in eq. (11) rounding to eight significant figures, we have

$$p^{[n_f]}_{gg,0}(x) = -8308.6173\, L_0^3/x - \left(106911.99 + 996.38304\, n_f\right) L_0^2/x$$

$$+ \left(144 - 27.786008\, n_f + 0.79012346\, n_f^2\right) L_0^6 - \left(144 + 162.08066\, n_f - 14.380247\, n_f^2\right) L_0^5$$
$$+ \left(26165.784 - 3344.7551 n_f + 91.522635\, n_f^2 - 0.19753086\, n_f^3\right) L_0^4$$
$$+ \left(247.55054\, n_f - 40.559671\, n_f^2 + 1.5802469\, n_f^3\right) x_1 L_1^3$$
$$+ \left(56.460905\, n_f - 3.6213992\, n_f^2\right) x_1 L_1^4 + P^{(3)-/+}_{\mathrm{gg},\,x\to 1}(x) \tag{13}$$

with $P^{(3)}_{\mathrm{gg},\,x\to 1}(x)$ given by eq. (10). The additional superscript $-/+$ indicates that -0.2 in eq. (11) is used for the approximations A, and $+0.2$ for the approximations B in

$$\begin{aligned}
p^{[3]}_{\mathrm{gg,A}}(x) = &-421311\, x_1 L_0/x - 325557\, x_1/x + 1679790\, x_1 - 1456863\, x_1 x + 3246307\, x_1 L_0 \\
&+ 2026324\, L_0^2 + 549188\, L_0^3 + 8337\, x_1 L_1 + 26718\, x_1 L_1^2 - 27049\, x_1^2 L_1^3 , \\
p^{[3]}_{\mathrm{gg,B}}(x) = &-700113\, x_1 L_0/x - 2300581\, x_1/x + 896407\, x_1(1+2x) - 162733\, x_1 x^2 \\
&- 2661862\, x_1 L_0 + 196759\, L_0^2 - 260607\, L_0^3 + 84068\, x_1 L_1 + 346318\, x_1 L_1^2 \\
&+ 315725\, L_0 L_1^2 ,
\end{aligned} \tag{14}$$

$$\begin{aligned}
p^{[4]}_{\mathrm{gg,A}}(x) = &-437084\, x_1 L_0/x - 361570\, x_1/x + 1696070\, x_1 - 1457385\, x_1 x + 3195104\, x_1 L_0 \\
&+ 2009021\, L_0^2 + 544380\, L_0^3 + 9938\, x_1 L_1 + 24376\, x_1 L_1^2 - 22143\, x_1^2 L_1^3 , \\
p^{[4]}_{\mathrm{gg,B}}(x) = &-706649\, x_1 L_0/x - 2274637\, x_1/x + 836544\, x_1(1+2x) - 199929\, x_1 x^2 \\
&- 2683760\, x_1 L_0 + 168802\, L_0^2 - 250799\, L_0^3 + 36967\, x_1 L_1 + 24530\, x_1 L_1^2 \\
&- 71470\, x_1^2 L_1^2 ,
\end{aligned} \tag{15}$$

$$\begin{aligned}
p^{[5]}_{\mathrm{gg,A}}(x) = &-439426\, x_1 L_0/x - 293679\, x_1/x + 1916281\, x_1 - 1615883\, x_1 x + 3648786\, x_1 L_0 \\
&+ 2166231\, L_0^2 + 594588\, L_0^3 + 50406\, x_1 L_1 + 24692\, x_1 L_1^2 + 174067\, x_1^2 L_1 , \\
p^{[5]}_{\mathrm{gg,B}}(x) = &-705978\, x_1 L_0/x - 2192234\, x_1/x + 1730508\, x_1 x + 353143 x_1(2-x^2) \\
&- 2602682\, x_1 L_0 + 178960\, L_0^2 - 218133\, L_0^3 + 2285\, x_1 L_1 + 19295\, x_1 L_1^2 \\
&- 13719\, x_1^2 L_1^2 .
\end{aligned} \tag{16}$$

The error bands above lead to precise numerical predictions for $\gamma^{(3)}_{\mathrm{gg}}$ at higher values of N such as

$$-\gamma^{(3)}_{\mathrm{gg}}(N{=}22) = 23990.457275(20), \quad 6396.872080(20), \quad -8123.349380(20) \tag{17}$$

for $n_f = 3, 4, 5$, where the brackets indicate a conservative uncertainty of the last two digits.

In order to illustrate the size and uncertainties of the present N^{3}LO contributions to the evolution of the gluon PDF, we adopt the reference point of ref. [4] with $n_f = 4$, $\alpha_s(\mu_0^2) = 0.2$ and

$$\begin{aligned}
xq_{\mathrm{s}}(x,\mu_0^2) &= 0.6\, x^{-0.3}(1-x)^{3.5}\left(1+5.0\, x^{0.8}\right), \\
xg(x,\mu_0^2) &= 1.6\, x^{-0.3}(1-x)^{4.5}\left(1-0.6\, x^{0.3}\right).
\end{aligned} \tag{18}$$

The resulting N^{2}LO and N^{3}LO contributions to the convolution $[P_{\mathrm{gg}} \otimes g](x)$ are shown in the right part of Fig. 2. In order to render these small effects visible, we have normalized these corrections to the NLO results, which however leads to an artificial singularity slightly above $x = 0.03$ due to a sign change at NLO. Except at the smallest values of x, the N^{3}LO corrections are below 1%. Their uncertainties are negligible at $x > 10^{-4}$. Even at $x = 10^{-5}$, the N^{3}LO effect amounts to only about 1.5% with an uncertainty of less than ± 1%.

Combining our above results with those for $P^{(3)}_{\mathrm{gq}}$ in ref. [14], in a manner that the uncertainties add up at small x, we are finally able to evaluate the N^{3}LO contributions to the scale derivative (1) of the gluon PDF at the above reference point. The relative size of the N^{2}LO and N^{3}LO contributions to $\dot g \equiv dg/d\ln\mu^2$ is shown in the left panel of Fig. 3. Both the N^{3}LO corrections and their uncertainties are below 1% at $x > 10^{-4}$, reaching (2 ± 1)% at $x = 10^{-5}$.

So far we have identified the renormalization scale μ_{r} with the factorization scale $\mu_{\mathrm{f}} \equiv \mu$. The expansion in eq. (1) is readily expanded to $\mu_{\mathrm{r}} \neq \mu_{\mathrm{f}}$, see, e.g., eq. (2.9) of ref. [48] for the expression to order α_s^5. The scale stability of $\dot g$ is illustrated in the right panel of Fig. 3 by the quantity

$$\Delta_{\mu_{\mathrm{r}}}\, \dot g \;\equiv\; \frac{\max[\,\dot g(x,\mu_{\mathrm{r}}^2 = \lambda\,\mu_{\mathrm{f}}^2)] - \min[\,\dot g(x,\mu_{\mathrm{r}}^2 = \lambda\,\mu_{\mathrm{f}}^2)]}{2|\,\mathrm{average}[\,\dot g(x,\mu_r^2 = \lambda\,\mu_{\mathrm{f}}^2)]\,|} \tag{19}$$

for the conventional range $\lambda = 1/4 \ldots 4$. At $x > 10^{-4}$ this N^{3}LO scale uncertainty is below 1%, except close to the sign change of $\dot g$ at $x \simeq 0.07$. It reaches (3 ± 1)% at $x = 10^{-5}$. This is very similar to the result for the quark PDF in Fig. 3 of ref. [14], where the improvement on the N^{2}LO uncertainty is much more impressive since the latter is much larger than in the present gluon case.

With this article, we have completed the computation of the moments to $N = 20$ of the four-loop (N^{3}LO) splitting functions for the evolution of the flavour singlet PDFs in the $\overline{\mathrm{MS}}$ scheme. We have combined these moments with knowledge on the $x \to 0$ and $x \to 1$ limits to construct approximate expressions for $P^{(3)}_{\mathrm{ik}}(x)$ that should be sufficient for most high-scale applications. For example, the N^{3}LO effects on the scale dependence $df/d\ln\mu^2$, $f = q_{\mathrm{s}}, g$ are below 1% with an irrelevant approximation error down to $x \gtrsim 10^{-4}$ at a standard reference point with $\mu^2 \simeq 25 \ldots 50$ GeV^2, as shown in

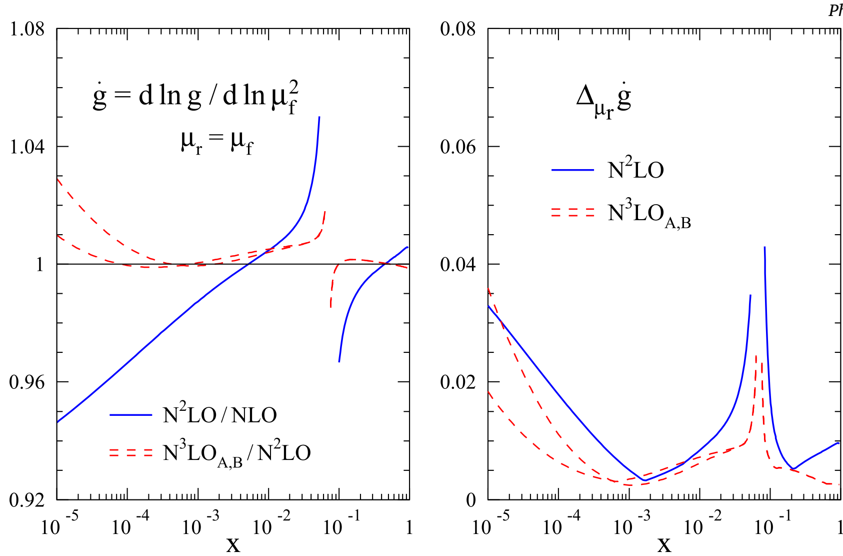

Fig. 3. Left: the relative N^{2}LO and N^{3}LO corrections to the scale derivative of the gluon PDF g at the reference point with $n_f = 4$ and $\alpha_s(\mu_0^2) = 0.2$. Right: the renormalization-scale uncertainties of these results, as estimated using eq. (19). Note that $dg/d\ln\mu^2$ changes sign close to $x = 0.07$, which leads to (irrelevant) singularities in both the relative corrections and the relative scale uncertainty in eq. (19).

the left parts of Fig. 3 of ref. [13] and Fig. 3 above. The remaining large uncertainties of $P_{\rm ik}^{(3)}(x)$ for $x \to 0$ would shrink dramatically if all small-x logarithms $x^{-1} \ln^{\ell} x$ were calculated.

Declaration of competing interest

The authors declare that they have no known competing financial interests or personal relationships that could have appeared to influence the work reported in this paper.

Acknowledgements

This work has been supported by the UKRI FLF Mr/S03479x/1; the STFC Consolidated Grants ST/X000494/1 and ST/T000988/1; the EU Marie Sklodowska-Curie grant 101104792; the DFG through the Research Unit FOR 2926, project number 40824754, and DFG grant MO 1801/4-2, and the ERC Advanced Grant 101095857.

Appendix A. Mellin moments of $P_{\rm gg}^{(3)}$

The four-loop anomalous dimensions $\gamma_{\rm gg}^{(3)}(N)$ at even $2 \le N \le 10$ have been already been obtained in refs. [10,11] for a general compact simple gauge group. Here we report the corresponding expressions for $12 \le N \le 20$. The numerical values in QCD have been given in eq. (5) above.

The quadratic Casimir invariants in SU(n_c) are $C_A = n_c$ and $C_F = (n_c^2 - 1)/(2n_c)$. The quartic group invariants are products of two symmetrized traces of four generators T_r^a,

$$d_r^{abcd} \;=\; \frac{1}{6}\,\mathrm{Tr}\,(T_r^a T_r^b T_r^c T_r^d \;+\; \text{five } bcd \text{ permutations})\,, \tag{A.1}$$

in the fundamental (R) or adjoint (A) representation, which leads to ($n_a = n_c^2 - 1$)

$$\frac{d_{AA}^{(4)}}{n_a} \;=\; \frac{1}{24}\, n_c^2 (n_c^2 + 36)\;, \quad \frac{d_{RA}^{(4)}}{n_a} \;=\; \frac{1}{48}\, n_c (n_c^2 + 6)\;, \quad \frac{d_{RR}^{(4)}}{n_a} \;=\; \frac{(n_c^4 - 6\,n_c^2 + 18)}{96\,n_c^2}\;, \tag{A.2}$$

and hence $d_A^{abcd}\, d_A^{abcd}/n_a = 135/8$, $d_R^{abcd}\, d_A^{abcd}/n_a = 15/16$ and $d_R^{abcd}\, d_R^{abcd}/n_a = 5/96$ in QCD.

$$\begin{aligned}
\gamma_{\rm gg}^{(3)}(N=12) \;=\; & C_A^4 \Big(\frac{4269168088456708901854865597025 59}{43501074073501680299664 0000000} + \frac{2858733158927526553}{4499203191210000}\,\zeta_3 \\
& - \frac{7173493238}{10061415}\,\zeta_5 \Big) + \frac{d_{AA}^{(4)}}{n_a} \Big(\frac{5186984525115894967}{3012146177040000} + \frac{11837685988559}{2112897150}\,\zeta_3 - \frac{28693972952}{3353805}\,\zeta_5 \Big) \\
& + n_f\, C_A^3 \Big(- \frac{55171996036371050045998366332119}{1028303777854691734556160 00000} - \frac{2216417127123463709}{2304353803752000}\,\zeta_3 \\
& + \frac{28951453}{53235}\,\zeta_4 + \frac{8698336}{31941}\,\zeta_5 \Big) + n_f\, C_F\, C_A^2 \Big(- \frac{31891030785065733878575519402109}{8911966074740661699486720 0000} \\
& + \frac{2106337731062115325 7}{57032756642862000}\,\zeta_3 - \frac{15914749031}{29066310}\,\zeta_4 + \frac{25095032}{39039}\,\zeta_5 \Big) \\
& + n_f\, C_F^2\, C_A \Big(\frac{2879456567418214942254486948055493}{1213141381924072573842629760 0000} + \frac{227712212175109611 1}{3802183776190800}\,\zeta_3
\end{aligned}$$

$$
\begin{aligned}
&+ \frac{18263117221}{3517023510}\,\zeta_4 - \frac{115425482}{117117}\,\zeta_5\Big) + n_f\, C_F^3 \Big(- \frac{18091355530448422177420899052043 3}{1213141381924072573842629760000 0}\\
&- \frac{1713716843924069}{475272972023850}\,\zeta_3 - \frac{2642589184}{1758511755}\,\zeta_4 + \frac{16220}{13013}\,\zeta_5\Big) + n_f\, \frac{d_{RA}^{(4)}}{n_a} \Big(\frac{378251047050369859609}{662672158948800000}\\
&+ \frac{476371067828641}{852201850500}\,\zeta_3 - \frac{27773168}{16731}\,\zeta_5\Big) + n_f^2\, C_A^2 \Big(\frac{43776212234240781257735569}{6277800841603734643200000}\\
&+ \frac{240437709082559}{949596347700}\,\zeta_3 - \frac{57902906}{585585}\,\zeta_4 - \frac{8620}{169}\,\zeta_5\Big) + n_f^2\, C_F C_A \Big(\frac{305917755861829264698421948 3}{403976484157200324289920 00}\\
&- \frac{3778891871983}{15826605795}\,\zeta_3 + \frac{58210216}{585585}\,\zeta_4\Big) + n_f^2\, C_F^2 \Big(- \frac{285515959062759190315953765 97}{240702655143665193222744000 0}\\
&+ \frac{317531792566}{15826605795}\,\zeta_3 - \frac{61462}{117117}\,\zeta_4\Big) + n_f^2\, \frac{d_{RR}^{(4)}}{n_a} \Big(\frac{5121825047548437461}{7888954273200000} + \frac{812056934692}{553377825}\,\zeta_3\\
&- \frac{413760}{169}\,\zeta_5\Big) + n_f^3\, C_A \Big(- \frac{504853821441288677}{410635847828606400} + \frac{809864}{110565}\,\zeta_3\Big)\\
&+ n_f^3\, C_F \Big(- \frac{6113543346521554934099}{1233139451029305019200 0} - \frac{24964}{351351}\,\zeta_3\Big),
\end{aligned}
\tag{A.3}
$$

$$
\begin{aligned}
\gamma_{\rm gg}^{(3)}(N=14) = {} & C_A^4 \Big(\frac{35303028582726265111669086796098 71}{33209268706590950113620480000000} + \frac{392576018133364531}{527175090288000}\,\zeta_3\\
&- \frac{12182898853}{14407470}\,\zeta_5\Big) + \frac{d_{AA}^{(4)}}{n_a} \Big(\frac{7388026987231247233447}{3568234702032000000} + \frac{7007627407900661}{1058949045000}\,\zeta_3\\
&- \frac{24365797706}{2401245}\,\zeta_5\Big) + n_f\, C_A^3 \Big(- \frac{113594703594760740723691396139053}{19821877556734726881408000000 0}\\
&- \frac{543858408413511329}{524956339908000}\,\zeta_3 + \frac{81775856}{143325}\,\zeta_4 + \frac{294336388}{945945}\,\zeta_5\Big)\\
&+ n_f\, C_F C_A^2 \Big(- \frac{28644681812359432810528968921761}{7362411663930041413094400000 0} + \frac{61123089029529077743}{153549729423090000}\,\zeta_3\\
&- \frac{189827271499}{331080750}\,\zeta_4 + \frac{70425496}{105105}\,\zeta_5\Big) + n_f\, C_F^2 C_A \Big(\frac{636323206729104618703233441133681 3}{2512422980316126632218464000000 00}\\
&+ \frac{729557540910110873}{1163255525932500}\,\zeta_3 + \frac{17085172697}{4304049750}\,\zeta_4 - \frac{326322424}{315315}\,\zeta_5\Big)\\
&+ n_f\, C_F^3 \Big(- \frac{41661188443381861417961826412 73}{24539067426077870938272000000 0} - \frac{10174644862216}{3776803655625}\,\zeta_3 - \frac{505959889}{430404975}\,\zeta_4\\
&+ \frac{2816}{3185}\,\zeta_5\Big) + n_f\, \frac{d_{RA}^{(4)}}{n_a} \Big(\frac{16222306083794825031617}{3189109764941100000 0} + \frac{21688516374213961}{82024428110625}\,\zeta_3 - \frac{399720544}{315315}\,\zeta_5\Big)\\
&+ n_f^2\, C_A^2 \Big(\frac{8626478681237589833615375 9}{715074947934153206400000 0} + \frac{2455639519261343}{8948119430250}\,\zeta_3 - \frac{163551712}{1576575}\,\zeta_4 - \frac{16432}{245}\,\zeta_5\Big)\\
&+ n_f^2\, C_F C_A \Big(\frac{4787481590605144814770575829}{5975983493449708939200000 0} - \frac{371371561826}{1489863375}\,\zeta_3 + \frac{164162696}{1576575}\,\zeta_4\Big)\\
&+ n_f^2\, C_F^2 \Big(- \frac{4739513395285756865207465 71}{396531404721610895236500 00} + \frac{385728471251}{19368223875}\,\zeta_3 - \frac{55544}{143325}\,\zeta_4\Big)\\
&+ n_f^3\, C_A \Big(- \frac{49815330459045199}{38655875938680000} + \frac{718924}{93555}\,\zeta_3\Big) + n_f^3\, C_F \Big(- \frac{3907253297496328220297}{7545433703850642600000}\\
&- \frac{22472}{429975}\,\zeta_3\Big) + n_f^2\, \frac{d_{RR}^{(4)}}{n_a} \Big(\frac{4485052909723377974579}{5315182941568500000} + \frac{226041368622508}{114719479875}\,\zeta_3 - \frac{788736}{245}\,\zeta_5\Big),
\end{aligned}
\tag{A.4}
$$

$$
\begin{aligned}
\gamma_{\rm gg}^{(3)}(N=16) = {} & C_A^4 \Big(\frac{15337182291951433616165281475248927995540971534167}{134923393479242648742469916142961946419200000000}\\
&+ \frac{5529754419565844478534458563}{65206103253826264329600000}\,\zeta_3 - \frac{38027329168168}{39093069015}\,\zeta_5\Big)\\
&+ \frac{d_{AA}^{(4)}}{n_a} \Big(\frac{17225198856494540525364768331}{7156940604431871052800000} + \frac{4280088643520652417443}{563503134009816000}\,\zeta_3\\
&- \frac{152109316672672}{13031023005}\,\zeta_5\Big) + n_f\, C_A^3 \Big(- \frac{897432462848236045017850628184670314114341}{147855318661037466570144214833152000000}\\
&- \frac{133102211488321772967121}{120260238076679500800}\,\zeta_3 + \frac{11241734927}{18935280}\,\zeta_4 + \frac{16593150641}{46864818}\,\zeta_5\Big)\\
&+ n_f\, C_F C_A^2 \Big(- \frac{26847608088981105116818871646074617292318363}{64633896443253521100663132819849216000000}\\
&+ \frac{236351484521633019349663}{558351105356011968000}\,\zeta_3 - \frac{10549880344093}{17704486800}\,\zeta_4 + \frac{10826183435}{15621606}\,\zeta_5\Big)\\
&+ n_f\, C_F^2 C_A \Big(\frac{3820884848912654785490648965626200547231253}{143630888098500782466814029515522048000000}\\
&+ \frac{74860657727420155363}{114839799538464000}\,\zeta_3 + \frac{160275239209}{50988921984}\,\zeta_4 - \frac{22442950375}{20828808}\,\zeta_5\Big)
\end{aligned}
$$

$$
\begin{aligned}
&+ n_f\, C_F^3 \Big(- \frac{432465293017180154359501484955972282652531}{235032350702740076729684119344906240000000} - \frac{375374254371104406 1}{180210146968051200 0}\, \zeta_3 \\
&- \frac{1209091491169}{1274723049600}\, \zeta_4 + \frac{20639}{31212}\, \zeta_5 \Big) + n_f\, \frac{d_{RA}^{(4)}}{n_a} \Big(\frac{412776185633813536481909239}{1022420086347410150400000} \\
&- \frac{18868730583338146213}{140875783502454000}\, \zeta_3 - \frac{5575791757}{7810803}\, \zeta_5 \Big) \\
&+ n_f^2\, C_A^2 \Big(\frac{14114230399879187349140102339657 53}{804507685457448143197458432000 00} + \frac{679370984698281247}{2296795990769280}\, \zeta_3 \\
&- \frac{11241734927}{104144040}\, \zeta_4 - \frac{1334035}{15606}\, \zeta_5 \Big) + n_f^2\, C_F\, C_A \Big(\frac{265603320468239150618251481266503761}{316516309392830312337971503104 0000} \\
&- \frac{1482304546167539}{5736253723200}\, \zeta_3 + \frac{8454580201}{78108030}\, \zeta_4 \Big) \\
&+ n_f^2\, C_F^2 \Big(- \frac{115012852022058117591081254974378254 19}{956582623942776055065869431603200000} + \frac{113706461016607}{5736253723200}\, \zeta_3 - \frac{93023}{312120}\, \zeta_4 \Big) \\
&+ n_f^2\, \frac{d_{RR}^{(4)}}{n_a} \Big(\frac{635174597191194864438483 13}{596411717035989254400 00} + \frac{7173470647621241}{2814700969080}\, \zeta_3 - \frac{10672280}{2601}\, \zeta_5 \Big) \\
&+ n_f^3\, C_A \Big(- \frac{1696185564468333948773}{1265075231715719424000} + \frac{680336}{85085}\, \zeta_3 \Big) \\
&+ n_f^3\, C_F \Big(- \frac{275863419549706106273826313 9}{516666845234553538516992000 0} - \frac{18769}{468180}\, \zeta_3 \Big)
\end{aligned}
\tag{A.5}
$$

$$
\begin{aligned}
\gamma_{\mathrm{gg}}^{(3)}(N=18) = {}& C_A^4 \Big(\frac{61382152389353026983139106547799892257240744 5587423}{50964657015912963136878325252991069237207040 0000} \\
&+ \frac{26004327721023621741020519 29}{27470763486767531522592 00}\, \zeta_3 - \frac{7132610803355}{6511002498}\, \zeta_5 \Big) \\
&+ \frac{d_{AA}^{(4)}}{n_a} \Big(\frac{104905372164432030240631629 1}{383787218983943174400000} + \frac{2277808717857396553}{266625552293100}\, \zeta_3 - \frac{14265221606710}{1085167083}\, \zeta_5 \Big) \\
&+ n_f\, C_A^3 \Big(- \frac{509024511103109450829223366317191978537219 39}{796405627194410643944693077718056857600 00} \\
&- \frac{932396716084659320721077653}{79311195281476689410880 0}\, \zeta_3 + \frac{46298577401}{75393045}\, \zeta_4 + \frac{31516663202}{78567489}\, \zeta_5 \Big) \\
&+ n_f\, C_F\, C_A^2 \Big(- \frac{4472469837937412890257391830178132693234847257}{1020789752316645388865618508344969702400000 0} \\
&+ \frac{1341599225293336415059231 73}{30095766066631779463950 0}\, \zeta_3 - \frac{87339087634793}{141814317645}\, \zeta_4 + \frac{354751643702}{497594097}\, \zeta_5 \Big) \\
&+ n_f\, C_F^2\, C_A \Big(\frac{6479793102254135084604771445003585679812041503 83}{2342712481566701167446594476651705467008000000} \\
&+ \frac{14181226205372837135476 19}{2104599025638585976500}\, \zeta_3 + \frac{30822057470944}{12054216999825}\, \zeta_4 - \frac{554803942604}{497594097}\, \zeta_5 \Big) \\
&+ n_f\, C_F^3 \Big(- \frac{70301841538977369648349286711177952437421103729}{3620555653330356349690191463916272085376000000} \\
&- \frac{26374016931923364628}{15943932012413530125}\, \zeta_3 - \frac{9447656272424}{12054216999825}\, \zeta_4 + \frac{85184}{165699}\, \zeta_5 \Big) \\
&+ n_f\, \frac{d_{RA}^{(4)}}{n_a} \Big(\frac{580668376095736761345039157}{224145942006932225280000 0} - \frac{28798161501291573012959}{45770542059947304600}\, \zeta_3 \\
&- \frac{4582985696}{497594097}\, \zeta_5 \Big) + n_f^2\, C_A^2 \Big(\frac{728050914273682280104737537321912140 9}{310179343928745969019165270487040000} \\
&+ \frac{827826218263460428211}{2606314582834162200}\, \zeta_3 - \frac{92597154802}{829323495}\, \zeta_4 - \frac{9320800}{87723}\, \zeta_5 \Big) \\
&+ n_f^2\, C_F\, C_A \Big(\frac{619976473559417663859944479698070705897}{7103660867653869736912133203564800000} - \frac{2224097820277294}{8345227153725}\, \zeta_3 \\
&+ \frac{278379603958}{2487970485}\, \zeta_4 \Big) + n_f^2\, C_F^2 \Big(- \frac{29450269754989290176205939653770867886633}{24378876140179624203365327137983948000 00} \\
&+ \frac{238194199445648}{12054216999825}\, \zeta_3 - \frac{587552}{2485485}\, \zeta_4 \Big) + n_f^2\, \frac{d_{RR}^{(4)}}{n_a} \Big(\frac{508929299629112028606527827567}{38754833372998581750912 0000} \\
&+ \frac{215307386311880818}{67242378298095}\, \zeta_3 - \frac{149132800}{29241}\, \zeta_5 \Big) + n_f^3\, C_A \Big(- \frac{25223004081586999165793 71}{18183735581517382836960 00} \\
&+ \frac{38224084}{4621617}\, \zeta_3 \Big) + n_f^3\, C_F \Big(- \frac{1204343230800942414809786168123}{2204707477283604289122906780000} - \frac{236672}{7456455}\, \zeta_3 \Big)
\end{aligned}
\tag{A.6}
$$

$$
\begin{aligned}
\gamma_{\mathrm{gg}}^{(3)}(N=20) = {}& C_A^4 \Big(\frac{5144251834605103174182091617560167230359326249647 79}{4058945420500549683002636643967438554777600000 00} \\
&+ \frac{763868116963839482143732249 7}{733568661605545473708000 0}\, \zeta_3 - \frac{31656671189543}{26062046010}\, \zeta_5 \Big)
\end{aligned}
$$

$$
\begin{aligned}
&+ \frac{d_{AA}^{(4)}}{n_a} \Big(\frac{3889870578491714739384956213923949}{12743201131463612604674880000000} + \frac{3934478309186512848349}{415641774465918000} \zeta_3 \\
&- \frac{63313342379086}{4343674335} \zeta_5 \Big) + n_f\, C_A^3 \Big(- \frac{7696997158537528664444481273199677690897905823 7}{1148363993582298686864055664639154995200000000} \\
&- \frac{10836873355305051655841337131}{871471120821396679584000 0} \zeta_3 + \frac{9758076254}{15431325} \zeta_4 + \frac{27649610258}{61108047} \zeta_5 \Big) \\
&+ n_f\, C_F\, C_A^2 \Big(- \frac{749824139308232425240266651394266714405252486 53}{163641869085477562878127932211079586816000000} \\
&+ \frac{9186348609399688537629418 7}{1971184678048397251440 00} \zeta_3 - \frac{71007716588687}{112031419500} \zeta_4 + \frac{74400774706}{101846745} \zeta_5 \Big) \\
&+ n_f\, C_F^2\, C_A \Big(\frac{443983882055224098441711364087734398081167795336 1}{155459775631203684734221535600525607475200000 00} \\
&+ \frac{72173478489957566802498 31}{10405952297389729080000} \zeta_3 + \frac{7914266258212}{3725044698375} \zeta_4 - \frac{116965983598}{101846745} \zeta_5 \Big) \\
&+ n_f\, C_F^3 \Big(- \frac{3094381649957022841504156804036910647244861938 73}{153440817506123117400010866307012287897600000 00} \\
&- \frac{10474380989917400036281}{780446422304229681000 0} \zeta_3 - \frac{9834028074797}{14900178793500} \zeta_4 + \frac{63236}{153615} \zeta_5 \Big) \\
&+ n_f\, \frac{d_{RA}^{(4)}}{n_a} \Big(\frac{674022797013987259099101796890 01}{876455462435506387289856000000} - \frac{441765899439254687602027 49}{36311296700891528316000} \zeta_3 \\
&+ \frac{85425608144}{101846745} \zeta_5 \Big) + n_f^2\, C_A^2 \Big(\frac{1764536196013068548482095881742080505698 9}{590479223355768555565639482023424000000} \\
&+ \frac{84681522145912460089 7}{248946227210280600 0} \zeta_3 - \frac{19516152508}{169744575} \zeta_4 - \frac{855884}{6615} \zeta_5 \Big) \\
&+ n_f^2\, C_F\, C_A \Big(\frac{180886718618128207734971949917107035583 27}{2003411650671357599240562528293760 00000} - \frac{1833909745247}{6698382075} \zeta_3 \\
&+ \frac{58646289362}{509233725} \zeta_4 \Big) + n_f^2\, C_F^2 \Big(- \frac{143611841677221812934598916644203681895721}{118423888684129138088442140561364480 00000} \\
&+ \frac{24036876714101}{1219105537650} \zeta_3 - \frac{442678}{2304225} \zeta_4 \Big) + n_f^2\, \frac{d_{RR}^{(4)}}{n_a} \Big(\frac{699386406780523342608190829371494 7}{440219675450561162706950400000 0} \\
&+ \frac{10728928931473261367}{2729673543972375} \zeta_3 - \frac{13694144}{2205} \zeta_5 \Big) + n_f^3\, C_A \Big(- \frac{17841393971051599645630 1}{124871427568676748960000} \\
&+ \frac{8385068}{984555} \zeta_3 \Big) + n_f^3\, C_F \Big(- \frac{1212255611189452111330310657173 7}{218018544709251271521568032000 00} - \frac{178084}{6912675} \zeta_3 \Big) .
\end{aligned}
\tag{A.7}
$$

FORM files with the results for $\gamma_{gg}(N)$ at even $N \leq 20$ and the partial all-N expressions in the main text have been deposited at the preprint server http://arXiv.org together with a FORTRAN subroutine of our approximations for the splitting function $P_{gg}^{(3)}(x)$ in eqs. (13) - (16). These files are also available from the authors upon request.

Data availability

No data was used for the research described in the article.

References

[1] A. Dainese, M. Mangano, A.B. Meyer, A. Nisati, G. Salam, M.A. Vesterinen, Report on the Physics at the HL-LHC, and Perspectives for the HE-LHC, CERN Yellow Report, 7/2019.
[2] R. Abdul Khalek, et al., Nucl. Phys. A 1026 (2022) 122447, arXiv:2103.05419.
[3] S. Moch, J.A.M. Vermaseren, A. Vogt, Nucl. Phys. B 688 (2004) 101–134, arXiv:hep-ph/0403192.
[4] A. Vogt, S. Moch, J.A.M. Vermaseren, Nucl. Phys. B 691 (2004) 129–181, arXiv:hep-ph/0404111.
[5] S. Moch, B. Ruijl, T. Ueda, J. Vermaseren, A. Vogt, J. High Energy Phys. 10 (2017) 041, arXiv:1707.08315.
[6] J. Davies, A. Vogt, B. Ruijl, T. Ueda, J.A.M. Vermaseren, Nucl. Phys. B 915 (2017) 335, arXiv:1610.07477.
[7] T. Gehrmann, A. von Manteuffel, V. Sotnikov, T.Z. Yang, J. High Energy Phys. 01 (2024) 029, arXiv:2308.07958.
[8] G. Falcioni, F. Herzog, S. Moch, J. Vermaseren, A. Vogt, Phys. Lett. B 848 (2024) 138351, arXiv:2310.01245.
[9] W.L. van Neerven, A. Vogt, Phys. Lett. B 490 (2000) 111, arXiv:hep-ph/0007362.
[10] S. Moch, B. Ruijl, T. Ueda, J.A.M. Vermaseren, A. Vogt, Phys. Lett. B 825 (2022) 136853, arXiv:2111.15561.
[11] S. Moch, B. Ruijl, T. Ueda, J. Vermaseren, A. Vogt, Phys. Lett. B 849 (2024) 138468, arXiv:2310.05744.
[12] G. Falcioni, F. Herzog, S. Moch, A. Vogt, Phys. Lett. B 842 (2023) 137944, arXiv:2302.07593.
[13] G. Falcioni, F. Herzog, S. Moch, A. Vogt, Phys. Lett. B 846 (2023) 138215, arXiv:2307.04158.
[14] G. Falcioni, F. Herzog, S. Moch, A. Pelloni, A. Vogt, Phys. Lett. B 856 (2024) 138906, arXiv:2404.09701.
[15] G. Falcioni, F. Herzog, J. High Energy Phys. 05 (2022) 177, arXiv:2203.11181.
[16] T. Gehrmann, A. von Manteuffel, T.Z. Yang, J. High Energy Phys. 04 (2023) 041, arXiv:2302.00022.
[17] G. Falcioni, F. Herzog, S. Moch, S. Van Thurenhout, arXiv:2409.02870.
[18] J.A. Dixon, J.C. Taylor, Nucl. Phys. B 78 (1974) 552.
[19] R. Hamberg, W.L. van Neerven, Nucl. Phys. B 379 (1992) 143.
[20] P. Nogueira, J. Comput. Phys. 105 (1993) 279.
[21] J.A.M. Vermaseren, New features of FORM, arXiv:math-ph/0010025.
[22] J. Kuipers, T. Ueda, J. Vermaseren, J. Vollinga, Comput. Phys. Commun. 184 (2013) 1453–1467, arXiv:1203.6543.
[23] B. Ruijl, T. Ueda, J. Vermaseren, FORM version 4.2, arXiv:1707.06453.
[24] T. van Ritbergen, A.N. Schellekens, J.A.M. Vermaseren, Int. J. Mod. Phys. A 14 (1999) 41–96, arXiv:hep-ph/9802376.

[25] B. Ruijl, T. Ueda, J. Vermaseren, Comput. Phys. Commun. 253 (2020) 107198, arXiv:1704.06650.
[26] J. Davies, A. Vogt, Phys. Lett. B 776 (2018) 189–194, arXiv:1711.05267.
[27] S. Moch, B. Ruijl, T. Ueda, J.A.M. Vermaseren, A. Vogt, Phys. Lett. B 782 (2018) 627–632, arXiv:1805.09638.
[28] J.A.M. Vermaseren, Int. J. Mod. Phys. A 14 (1999) 2037–2076, arXiv:hep-ph/9806280.
[29] J. Blümlein, S. Kurth, Phys. Rev. D 60 (1999) 014018, arXiv:hep-ph/9810241.
[30] J.A.M. Vermaseren, A. Vogt, S. Moch, Nucl. Phys. B 724 (2005) 3–182, arXiv:hep-ph/0504242.
[31] T. Gehrmann, A. von Manteuffel, V. Sotnikov, T.Z. Yang, Phys. Lett. B 849 (2024) 138427, arXiv:2310.12240.
[32] E. Remiddi, J.A.M. Vermaseren, Int. J. Mod. Phys. A 15 (2000) 725, arXiv:hep-ph/9905237.
[33] S. Moch, J.A.M. Vermaseren, Nucl. Phys. B 573 (2000) 853, arXiv:hep-ph/9912355.
[34] B. Ruijl, T. Ueda, J.A.M. Vermaseren, J. Davies, A. Vogt, PoS LL2016 (2016) 071, arXiv:1605.08408.
[35] J.M. Henn, G.P. Korchemsky, B. Mistlberger, J. High Energy Phys. 04 (2020) 018, arXiv:1911.10174.
[36] A. von Manteuffel, E. Panzer, R.M. Schabinger, Phys. Rev. Lett. 124 (2020) 162001, arXiv:2002.04617.
[37] G. Das, S. Moch, A. Vogt, J. High Energy Phys. 03 (2020) 116, arXiv:1912.12920.
[38] G. Das, S. Moch, A. Vogt, Phys. Lett. B 807 (2020) 135546, arXiv:2004.00563.
[39] Yu.L. Dokshitzer, G. Marchesini, G.P. Salam, Phys. Lett. B 634 (2006) 504, arXiv:hep-ph/0511302.
[40] G. Soar, S. Moch, J.A.M. Vermaseren, A. Vogt, Nucl. Phys. B 832 (2010) 152, arXiv:0912.0369.
[41] T. Jaroszewicz, Phys. Lett. B 116 (1982) 291.
[42] S. Catani, F. Fiorani, G. Marchesini, Nucl. Phys. B 336 (1990) 18.
[43] V.S. Fadin, L.N. Lipatov, Phys. Lett. B 429 (1998) 127, arXiv:hep-ph/9802290.
[44] M. Ciafaloni, G. Camici, Phys. Lett. B 430 (1998) 349, arXiv:hep-ph/9803389.
[45] M. Ciafaloni, D. Colferai, J. High Energy Phys. 09 (2005) 069, arXiv:hep-ph/0507106.
[46] M. Ciafaloni, D. Colferai, G.P. Salam, A.M. Stasto, Phys. Lett. B 635 (2006) 320, arXiv:hep-ph/0601200.
[47] J. Davies, C.H. Kom, S. Moch, A. Vogt, J. High Energy Phys. 08 (2022) 135, arXiv:2202.10362.
[48] W.L. van Neerven, A. Vogt, Nucl. Phys. B 603 (2001) 42–68, arXiv:hep-ph/0103123.